Optimum Shape for Buckling and Post-Buckling Behavior of a Laminated Composite Panel with I-type Stiffeners

Gwang-Rog LEE*
Graduate School, Department of Mechanical Engineering, Sungkyunkwan University, Kyunggi-do 440-746, Korea
Won-Ho Yang, Myung-Won Suh
School of Mechanical Engineering, Sungkyunkwan University, Kyunggi-do 440-746, Korea

A shape optimization of stiffener was conducted to increase buckling load or failure load with stiffened laminated composite panel of I-type under compression loading. Design variables are cap length, web length, and/or thickness under the constraint of volume constancy. The objective function is buckling load and failure load of post-buckling based on Tsai-Hill theory using ABAQUS 5.8 for analysis and Optimizer on Broydon-Fletcher Goldfarb-Sharno Method and Augmented Lagrange Multiplier Method. The effects of relative length of a web and a cap of stiffener on buckling load and failure load of post-buckling were investigated with the results of optimum design.

Key Words: Stiffened Composite Panel, Buckling, Post-Buckling, Buckling Load, Failure Load, Design Variable

1. Introduction

Fiber reinforced composites have been widely used in aerospace industries because they not only have better mechanical qualities than other metallic materials for specific strength and fatigue characteristic but also could be designed and manufactured according to user's target value of their strength by changing fiber orientations. In addition, fiber reinforced composites have been used for the light-weight of structure and the efficiency of materials. In these cases, the structure with stiffener consists of a panel or shell, and these structural elements have a characteristic with relatively low buckling stress compared with the static strength of material itself. On the other hand, a buckling does not mean ultimate failure. For this reason, many researchers have accomplished a buckling and post-buckling of the laminated composite panels with different stiffener configurations based on a failure theory. For example, previous works by Steven et al. (1994, 1995, and 1997) have identified failure initiation mechanisms for panels, which had I, J, and hat-stiffeners. Gurvich and Pipes (1995) used a multi-step failure approach to study the failure probability of laminated composite beams subjected to bending. Lin et al. (1998) presented a procedure for reliability analysis of laminated composite plates with random material constants and uncertain stacking sequences subject to the failure modes of buckling and/or first-ply failure. However there were few papers, which dealt with an optimization considering a failure criterion of post-buckling, because it is computation intensive to perform the optimization of composite that demands much iteration for nonlinear analysis.

Buckling of beams, plates, and flat stiffened panels show a stable behavior, which has no

* Corresponding Author,
E-mail : lkr288@hanmail.net
TEL : +82-31-290-7496; **FAX** : +82-31-290-5849
Fracture Mechanics Lab., School of Mechanical Engineering, Sungkyunkwan University, Suwon, Kyunggi-do 440-746, Korea. (Manuscript **Received** April 6, 2001; **Revised** June 27, 2002)

reduction of the supporting load during post-buckling, although a buckling occurs. On that ground, a slight buckling can be allowed for the effective design minimizing weight since the buckling does not always mean ultimate failure. Unlike isotropic materials, fiber reinforced composite materials can improve the effective modulus and strength by changing a fiber orientation, a stacking sequence, or a shape of stiffener. Composite material would be more effective in designing a construction than isotropic material because it is difficult to changing the radius of a curvature, boundary conditions, or material properties.

The objectives of this study are not only to investigate an optimum shape of I-type stiffened laminated composite panels considering a buckling load and a post-buckling failure strength to be objective functions, but also to study what effect changing components of I-type stiffener makes on a buckling load and a post-buckling failure load/strength based on Tsai-Hill theory. In order to solve computationally expensive problems effectively, approximate methods, such as a 3-order polynomial curve fitting method and the bi-cubic interpolation function of the least-square method are employed for the effective design of laminated composite panels by changing a length of web and cap, and a thickness of the stiffener. Consequently, buckling load or post-buckling failure load is improved in each case with a different design variable and a different objective function under axial compression loading.

2. Verification Between Experiment and Finite Element Analysis

2.1 Definition of analysis model

The specimen considered in this study is the Stiffened Laminated Composite Panel (SLCP) for the experimental buckling tests performed by Lee and Hong (1996). They were produced by a specialized manufacturer from HFG CU-125 NS graphite/epoxy composite. The specimen is characterized by a length of span of 100 mm, a length of width of 160 mm, and a longitudinal length of 250 mm in order that the buckling mode of the stiffener defined by a cap, a web, and a thickness have three-wavelengths of sine.

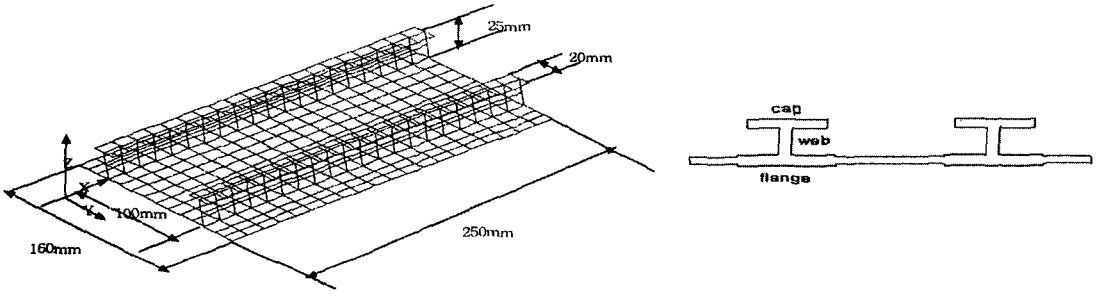

Fig. 1 Geometry of stiffened composite panel and finite element mesh

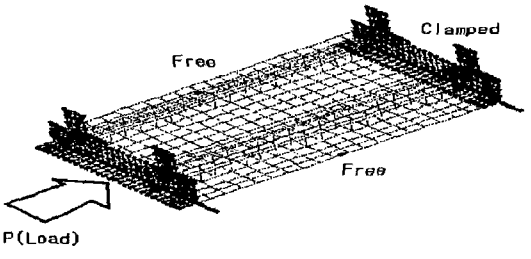

Fig. 2 Boundary condition and load condition (Lee and Hong, 1996)

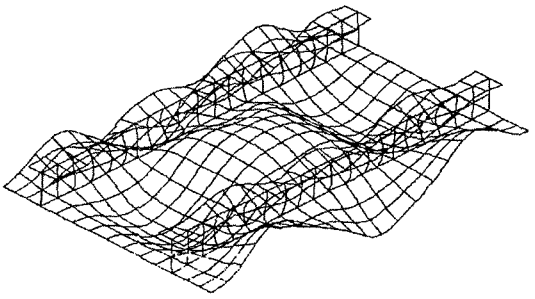

Fig. 3 Deformed shape of post-buckling analysis

Table 1 Stacking sequence of stiffened flat panel for comparison

Part	Stacking sequence
Panel	[0/90/±45]s
Stiffener cap	[0/90/45/0/-45]s
Stiffener web	[0/90/45/0/-45]s
Stiffener flange	[0/90/45/0/-45]s

Table 2 Material properties of HFG CU-125NS graphite/epoxy composite material (Lee and Hong, 1996)

Property	Symbol	Value
Elastic modulus in fiber-direction	E_1	130.0 GPa
Elastic moduli in transverse direction	E_2, E_3	10.0 GPa
Shear moduli in 1-2 and 1-3 planes	G_{12}, G_{13}	4.85 GPa
Shear modulus in 2-3 Plane	G_{23}	3.62 GPa
Poisson's ratios	ν_{12}, ν_{13}	0.31
	ν_{23}	0.52
Tensile strength in fiber-direction	X_T	1933 MPa
Compressive strength in fiber-direction	X_C	1051 MPa
Tensile strength in transverse direction	Y_T	51 MPa
Compressive strength in transverse direction	Y_C	141 MPa
Shear strength	S	61 MPa

Figure 1 shows load condition and finite element mesh made of 1405 nodes and 440 elements under axial compression. The dimensions of the panel clamped on the edge are given in Fig. 2. The thickness of panel is 0.125 mm. The skin consists of 8-ply, and each cap, web, and flange consists of 10-ply.

The ply stacking sequence of panel is [0/90/45]s, a quasi-isotropic ply. The ply stacking sequence of stiffener is [0/90/45/0/-45]s. The angle of ply (θ) designates counter clockwise as positive angle (+). The stacking sequence of flat panel for comparison is given in Table 2 and the material properties are reported in Table 1.

2.2 Methodology of finite element analysis (FEA)

The finite element analysis is accomplished to investigate the buckling and post-buckling behavior of panels under axial compression. MSC/PATRAN 7.0 (Pre-processor) and ABAQUS/Standard 5.8 (post-processor) are used.

Shell elements S8R with 8 nodes are selected. These elements feature six degrees of freedom at each node: three translations in the nodal x, y, and z directions and three rotations about the nodal x, y, and z axes. The shell elements use bending strain to get transverse shear deformation.

This study performed a linear eigenvalue analysis to determine the first buckling load (P_{cr}) and nonlinear Ritz method of ABAQUS to investigate the failure of post-buckling. First, following Koiter's suggestion (1994), the first linear buckling mode is employed as an imperfection shape because they yield the lowest critical load. Thus, the shape of imperfection with the amplitude corresponding to 10% of the panel thickness is applied in numerical model to decrease discrepancy between analytically predicted buckling loads and the ones observed in experiments. On the other hand, Tsai-Hill theory is introduced as a criterion of a failure because composite structures can undergo several local failure modes

commonly associated with local buckling instabilities. Although Tsai-Hill theory is inconsistent with the assumptions used in formulating the original von Mises, it has been successfully used for some composites due to ease evaluation of a failure. Thus, Tsai-Hill theory is applied in each step of nonlinear analysis, as the applied load is increased in order to monitor a failure of post-buckling behavior on nonlinear analysis. Tsai-Hill principle takes the following form :

$$\frac{\sigma_1^2}{S_L^2}-\frac{\sigma_1\sigma_2}{S_L^2}+\frac{\sigma_2^2}{S_T^2}+\frac{\tau_{12}^2}{S_{LT}^2}=1 \qquad (1)$$

where, σ_1, σ_2, and τ_{12} are the biaxial stress along the principal material axes, and S_L=longitudinal tensile strength, S_T=transverse tensile strength, S_{LT}=in-plane shear strength are strength.

Failure is avoided if the left-hand side of Tsai-Hill is less than 1, and failure is predicted if the left-hand side is great than 1.

2.3 Comparison between experimental and numerical results

In general, the SLCP has bending moments at the edge of panel due to the effect of geometric characteristics although in-plane loads are applied on it. Thus, transverse displacements appear even at the early stage of loading. Figure 3, for example, shows a shape of deformation when its step is judged to be the failure principle of nonlinear analysis by Tsai-Hill. In this case, Fig. 4 shows a transverse deflection of the center point of the panel. Figure 5 shows both the failure load and the difference of load-shortening displacement curve between experimental results performed by Lee and Hong (1996) and numerical results by ABAQUS. Consequently, the percentage of difference between them is less than about 5%.

3. Introduction of the Shape Optimization of I-Type Stiffener

3.1 Definition of problem of shape optimum design

In case the SLCP is optimized to improve the strength of the buckling and post-buckling, a symmetrical quasi-isotropic stacking sequence of skin is considered to be design variable in few cases, even though it is possible to change the fiber orientations of the composite, in that anisotropic composite panels with buckling modes results in energy concentration on local parts of the skin. In addition, the volume can be also limited due to reduction of weight. Thus, it is suitable to change a shape of the stiffener.

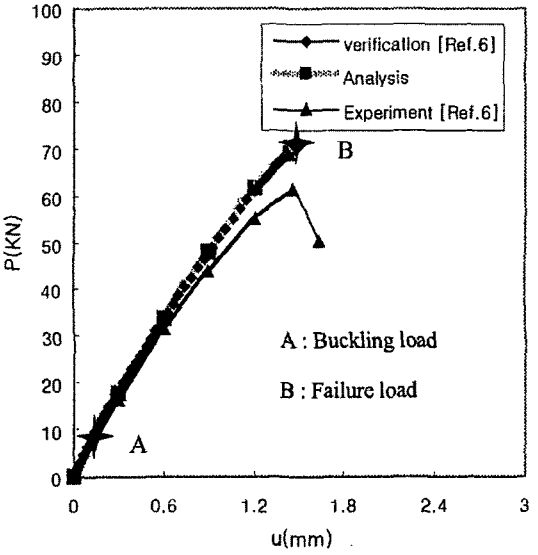

Fig. 4 Comparison of experiment results and analysis results of load-shortening displacement curve

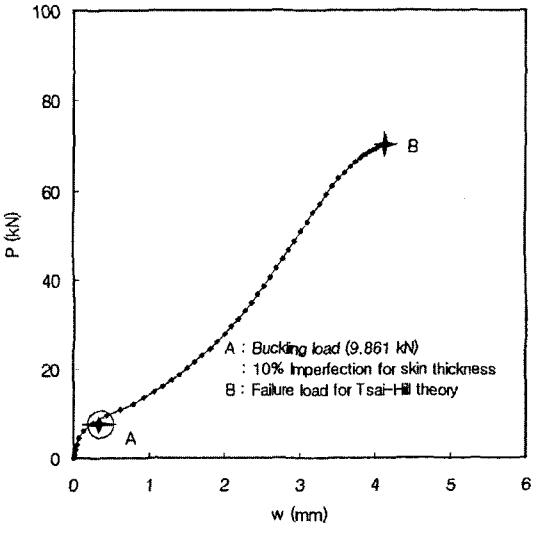

Fig. 5 Analysis results of load-transverse deflection curve

Dickson (1980) reported that I-type stiffened composite panels have the highest buckling load in I-type, J-type, Z-type, and C-type of SLCP. Therefore, this study performs maximizing the buckling load and the post-buckling load by changing the shape of the stiffener of the model based on I-type SLCP.

3.2 Objective function and constraints

This study investigates two objective functions. One is buckling load (P_{cr}) and the other is failure load of post-buckling (P_{T-H}) based on Tsai-Hill theory (Gibson, 1994). First, a buckling load obtained by eigenvalue analysis is considered as an objective function. The geometric constraint is the constant volume of I-type stiffener to research the optimum shape of I-type stiffener. Second, the failure load of post-buckling (P_{T-H}) obtained by nonlinear analysis is also considered an objective function to look over an optimum shape for P_{T-H} of post-buckling behavior. The geometric constraint is also the constant volume of I-type stiffener. Under constant volume, this study searched for how the optimum load of P_{cr} and P_{T-H} change the components of I-type stiffener such as the length of cap, the length of web, and the thickness of the stiffener. The purpose of this work is to detect a shape of I-type stiffener with P_{cr} or P_{T-H} under the I-type stiffener.

3.3 Design variable

The optimizations for four cases are accomplished according to objective function and design variables. Each case is listed below.

1. Case 1-1. : Optimization of buckling load (P_{cr}) for the stiffener, considering the change of the lengths of a cap and web under the constant thickness and volume.
2. Case 1-2. : Optimization of buckling load (P_{cr}) for the stiffener, considering the change of the thickness and lengths of a cap and web under the constant volume.
3. Case 2-1. : Optimization of post-buckling failure load (P_{T-H}) for the stiffener, considering the change of the lengths of a cap and web under the constant thickness and volume.
4. Case 2-2. : Optimization of post-buckling failure load (P_{T-H}) for the stiffener, considering the change of the thickness and lengths of a cap and web under the constant volume.

3.4 Methodology of optimum design

First, the optimization of buckling load is attained by maximizing P_{cr} obtained by eigenvalue analysis.

Next, for the optimization of post-buckling load, case 2-1 uses a predicted equation obtained by a curve fitting on the basis of polynomial form presenting objective function (P_{T-H}). On the other hand, case 2-2 employs bi-cubic interpolation methods to approximate the value of a function between known data points from datum based on nonlinear analysis for several design variables. This predicted data is found to be within 3% error, compared with P_{T-H} of nonlinear analysis.

Last, the optimizer is programmed using algorithms listed in Table 3 to associate with the results of ABAQUS for optimization.

3.5 Formulation of optimum problem

3.5.1 Optimum design for buckling load (P_{cr})

Case 1-1

$$\min_{\vec{x}} -P_{cr}(c, h) \tag{2}$$

Where c is the length of cap
h is the length of web
subject to
$c+h=45$ $t=1.25 \Rightarrow$ constant volume
$0<\vec{X}_i<45$ where $\vec{X}_i$=design variable (c, h)

Table 3 Algorithms of optimization

Strategy	Augmented Lagrange Multiplier Method
Optimizer	Broydon-Fletcher Goldfarb-Sharno Method
One-dimensional Search algorithm	Golden Section Method

Equation (2) means maximum value of P_{cr} as design variables (c, h) change in order to search for optimum shape.

Case 1-2

$$\min_{\vec{x}} -P_{cr}(c, h, t) \tag{3}$$

Where c is the length of cap
h is the length of web
t is the thickness of stiffener.

subject to

$t*(c+h)=56.25 \Rightarrow$ constant volume

$h=\frac{56.52}{t}-c>0$

$0<\vec{X}_i$ where $\vec{X}_i$=design variable (c, h, t).

Equation (3) means maximum value of P_{cr} as design variables (c, h, t) change in order to search for optimum shape.

3.5.2 Optimum design for post-buckling load (P_{T-H})

Case 2-1

$$\min_{\vec{x}} -P_{T-H}(c, h) \tag{4}$$

subject to

$c+h=45$ $t=1.25 \Rightarrow$ constant volume

$0<\vec{X}_i<45$ where $\vec{X}$=design variable (c, h).

$$\frac{\sigma_1^2}{S_L^2}-\frac{\sigma_1\sigma_2}{S_L^2}+\frac{\sigma_2^2}{S_T^2}+\frac{\tau_{12}^2}{S_{LT}^2}<1$$

Equation (4) means maximum value of P_{T-H} as design variables (c, h) change in order to search for optimum shape under the condition that Tsai-Hill theory is less than 1.

Case 2-2

$$\min_{\vec{x}} -P_{T-H}(c, h, t) \tag{5}$$

subject to

$t*(c+h)=56.25 \Rightarrow$ constant volume

$h=\frac{56.25}{t}-c>0$

$0<\vec{X}_i$ where $\vec{X}_i$=design variable (c, h, t).

$$\frac{\sigma_1^2}{S_L^2}-\frac{\sigma_1\sigma_2}{S_L^2}+\frac{\sigma_2^2}{S_T^2}+\frac{\tau_{12}^2}{S_{LT}^2}<1$$

Equation (5) means maximum value of P_{T-H} as design variables (c, h, t) change in order to search for optimum shape under the condition that the value of Tsai-Hill theory is less than 1 in each section-point of all element.

3.6 Flowchart for optimization

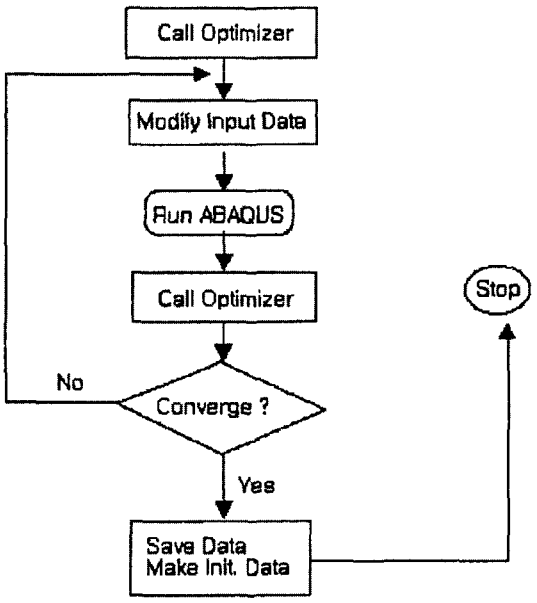

Fig. 6 Flowchart for optimization

Geometric input data of ABAQUS changes and continue to calculate the value of objective function in each iteration as shown in Fig. 6 until objective function has maximum value under constraint condition, in other words, until objective function violate constrains or could not search for better value any more, however design variables change.

3.7 The result of optimization

3.7.1 Case 1-1

Objective function is Pcr and design variables are the lengths of cap and web. In addition, case 1-1 is studied under both the constant thickness (1.25 mm) and the constant volume. The purpose of this case is to detect an optimum shape for maximizing buckling load under the constant volume of the stiffener. Figure 7 is a tendency of buckling load according to the variation of a length of cap (c) and a length of web (h) during optimization. The tendency indicates that the buckling load increases as the length of cap gets longer. The result of optimum design is $c=38.72$ mm $h=6.276$ mm, and this result corresponds to the trend of design variables (c, h) presented

in parameter study of Fig. 7. Therefore, the length of the cap is longer than the length of web in I-type stiffener under both the constant volume and the constant skin thickness, that is, the design variable c is more important than the design variable h for maximum P_{cr}. Maximum P_{cr} appears when c is 6 times higher than h.

3.7.2 Case 2-1

Objective function, P_{T-H} is calculated by inserting the stresses obtained from each step of nonlinear analysis into a failure criterion equation of Tsai-Hill which estimates 1 to be a failure, that is, if the value of the failure criterion from a section point of each node of panels exceed 1.

During this process, it is difficult to carry out the optimization due to iteration of P_{T-H} for optimum value in each step and time-consuming of nonlinear analysis. Thus, to overcome this hardship, case 2-1 employs a function of curve fitting of the least-square method using P_{T-H} at the regular intervals to obtain unknown values of function needed for each step of optimization, as shown in Fig. 8. Consequently, objective function could be obtained as design variables change, and the optimization is approximately accomplished. Figure 9 shows polynomial curve pitting of Fig. 8.

The result of optimum design is c=9.821 mm h=35.18 mm when c is 3.6 times higher than post-buckling. Figure 10 can be plotted by the two non-dimensional numbers, such as an aspect ratio (c/t) and a dimensionless quantity (P_{T-H}/P_{cr}). Fig. 10 indicates that P_{T-H} of the optimum shape not only is improved 1.5 times more than P_{T-H} before optimization but also has ability of load supporting 10 times more than P_{cr}.

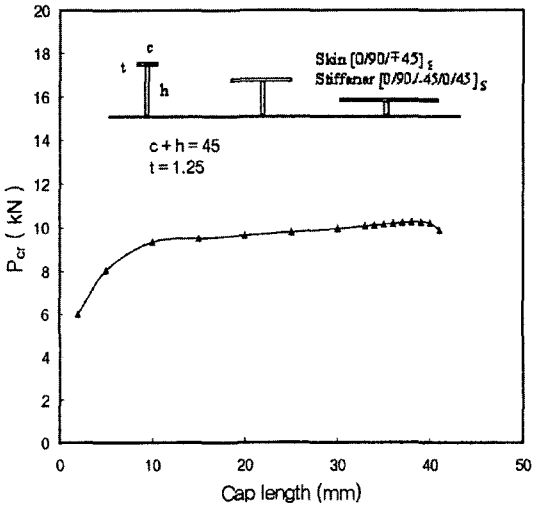

Fig. 7 Buckling load of eigenvalues analysis for variation of cap length (Effect of buckling load for stiffener shape)

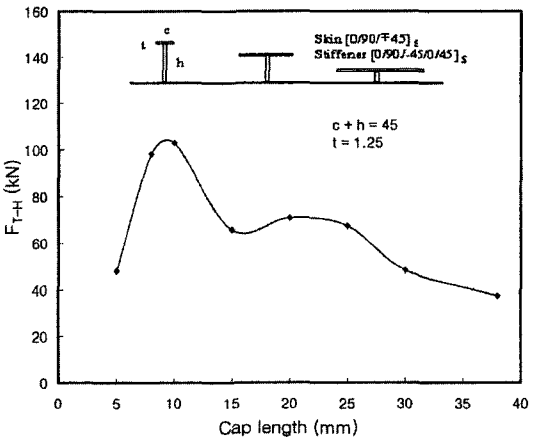

Fig. 8 Failure load of nonlinear analysis for variation of cap length (Effect of failure load for stiffener shape)

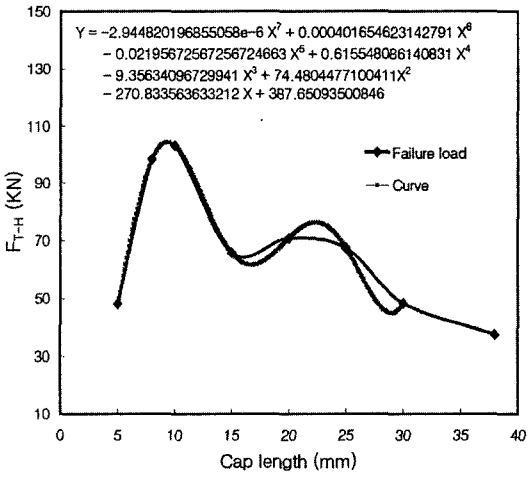

Fig. 9 Curve fitting for approximation of failure load (to optimize failure load of nonlinear analysis)

3.7.3 Case 1-2

Objective function is P_{cr} and design variables are a length of cap (c), a length of web (h) and a thickness (t). Figure 11 shows the tendency of Pcr versus design variables. The design variables are subjected to the condition of constant volume, $t \times (c+h) = 56.27\ mm^3$. This means that the total length of c and h is inverse proportion to a thickness (t). This correlation helps to investigate effects of each design variable for P_{cr}.

The result of optimum design is $c = 14.02$ mm $h = 10.90$ mm $t = 2.258$ mm, that is, the thickness (t) is increased when compared with original t. This explains that thickness t is also important for designing buckling load. Therefore, it is clear that the buckling load is as high as Case 1-1, in case c is longer than h according to the increase of t. Figure 12 shows variations for components of the stiffener during optimization.

3.7.4 Case 2-2

Objective function is P_{T-H} and design variables are a length of cap (c), a length of web (h), and thickness (t). The design variables are subjected to the condition of constant volume, $t \times (c+h) =$

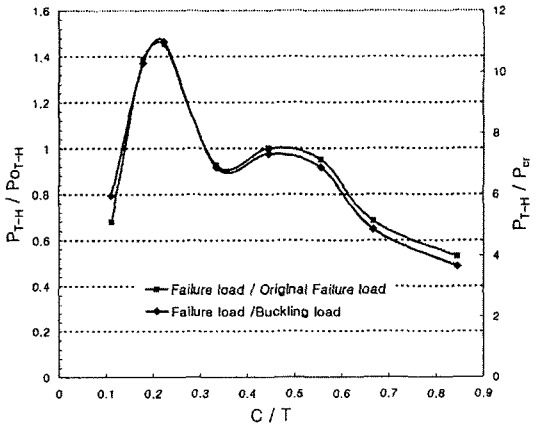

Fig. 10 Variation of nondimensional failure load for aspect ratio

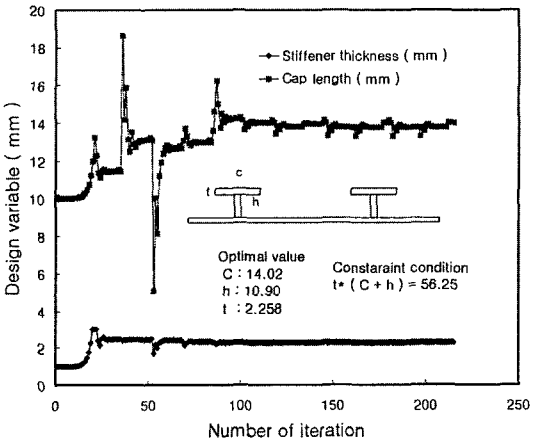

Fig. 12 Variation of design variable for iteration of buckling load-optimization

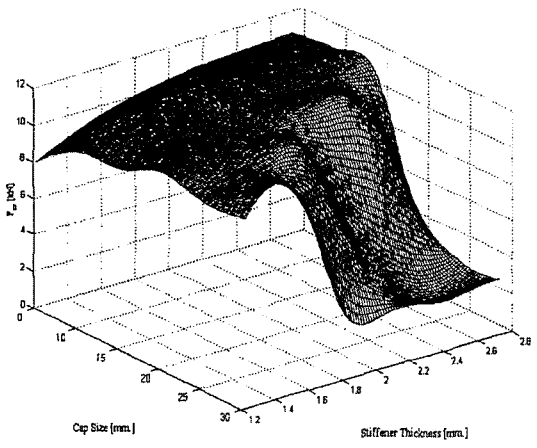

Fig. 11 Buckling load of eigenvalues analysis for variation of cap length and stiffener thickness

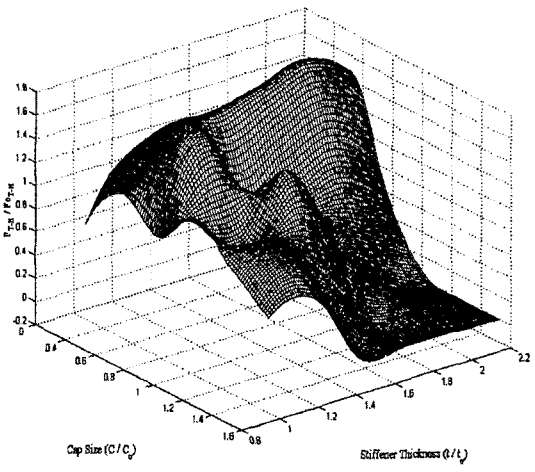

Fig. 13 Failure load of nonlinear analysis for variation of cap length and stiffener thickness

56.27mm^3. To overcome the computational expensiveness of nonlinear analysis, this case also employs a function of bi-cubic interpolation of the least-square method using P_{T-H} at the regular intervals to obtain the value of the function needed for iterations, as shown in Fig. 13. Figure 13-14 show 3-dimensional plotting and contour line of the objective function.

The result of optimum design is $c=10.24$ mm $h=13.39$ mm $t=2.38$ mm. For the optimum shape, the thickness (t) is increased when compared with original t. In addition, h must be longer than c for improving the post-buckling failure load like case 1-2. Therefore, it is predicted that the length of cap (c) would be a critical component of I-type stiffener for buckling load, and the length of web (h) would be for post-buckling failure load (P_{T-H}). Figure 15 shows the variations of components of stiffener during optimization. In short, P_{T-H} of the optimum shape is improved 1.78 time more than that of the original model and has the ability of supporting load 13 times more than P_{cr}. Graphically, Fig. 18 presents the optimum shape of the stiffener for P_{cr}, and Fig. 19 shows the optimum shape of stiffener for P_{T-H}.

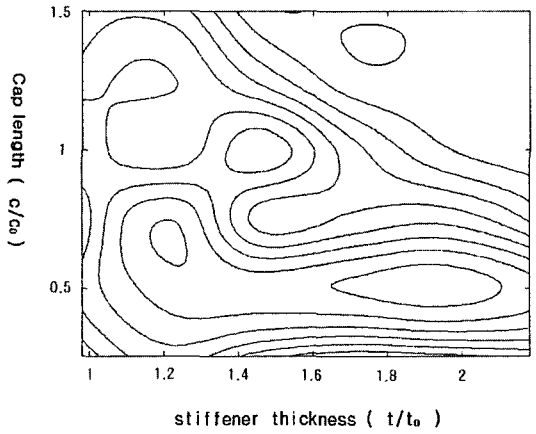

Fig. 14 Contour plot of failure load of nonlinear analysis for variation of cap length and stiffener thickness

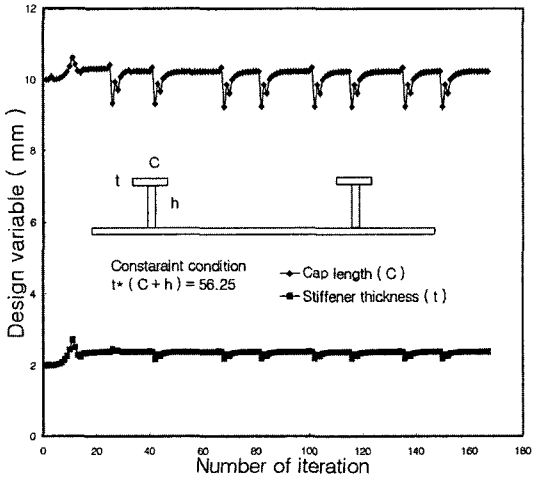

Fig. 15 Variation of cap length and stiffener thickness for iteration of failure load-optimization

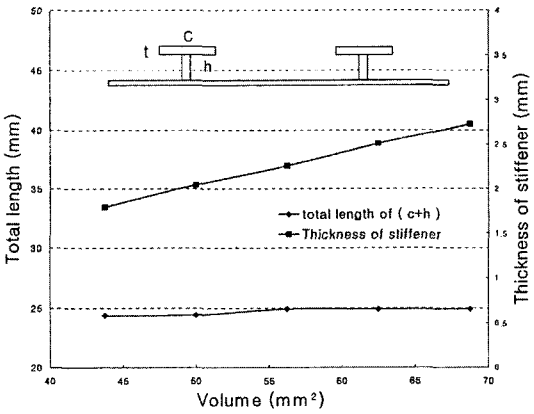

Fig. 16 Variation of thickness and total length for the increase of volume of stiffener

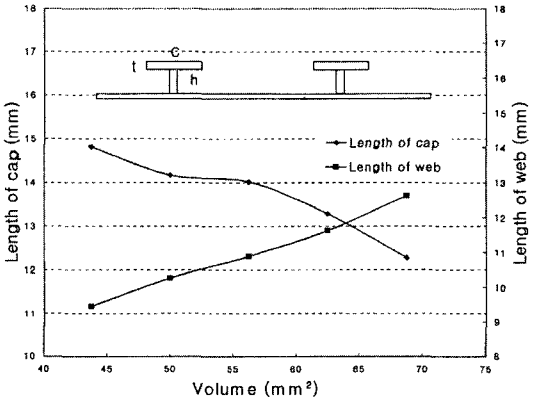

Fig. 17 Variation of length between cap and web for the increase of volume of stiffener

3.7.5 Optimization of P_{cr} as the volume of stiffener is raised

In case the optimization is accomplished as the volume of I-type stiffener is increased, it is seen that the total length of cap and web is almost constant although the thickness of the stiffener (t) is increased, as shown in Fig. 16. Therefore, if a designer intend to increase the buckling load through the volume-increase of I-type stiffener, the increase of t is more efficient than that of the total length of c and h because the optimum shape has the constant total length of c and h regardless of the increase of a little volume as shown in Figs. 17-18.

4. Conclusions

In this study, the optimization of I-type stiffened composite panels with constraints of volume was performed in view of buckling load and post-buckling failure load and then, we came up with the following three conclusions.

(1) The shape for optimum design of the stiffener are different between buckling load (P_{cr}) and post-buckling failure load (P_{T-H}). For example, the optimum shape of I-type stiffener for maximization of Pcr indicates that the length of

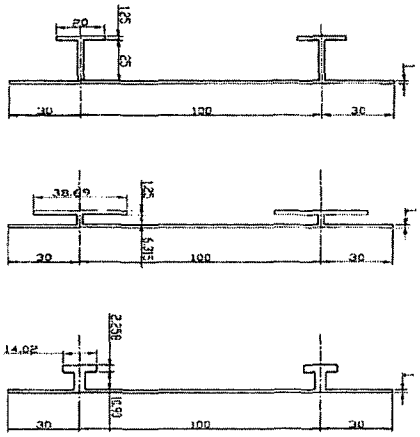

Original model

Optimal shape
(Consider cap and web)

Optimal shape
(Considering cap, web, and thickness)

Fig. 18 Shape of stiffener for buckling load

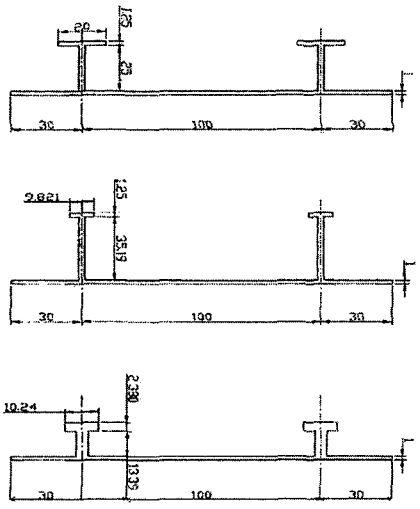

Original model

Optimal shape
(Consider cap and web)

Optimal shape
(Considering cap, web, and thickness)

Fig. 19 Shape of stiffener for failure load

cap is relatively longer than the length of web, while the optimum shape of I-type stiffener for maximization of P_{T-H} indicates that the length of web is relatively longer than the length of cap.

(2) If the volume of the stiffener is increased to elevate the P_{cr}, the increase of thickness of the stiffener is more effective than the increase of length of a cap and web because the total length of a cap and web for optimum shape is constant regardless of a volume change to some extent.

(3) This study uses approximate methods, such as curve fitting and interpolation function, to optimize objective function from nonlinear analysis. On the other hand, these results can be used for designing the load of buckling and post-buckling of I-type stiffened composite panels.

Acknowledgment

The authors are grateful for the support provided by a grant from the Korea Science & Engineering Foundation (KOSEF) and Safety and Structural Integrity Research Center at the Sungkyunkwan University.

References

Dickson, J. N., Cole, R. T. and Wang, J. T. S., 1980, "Design of Stiffened Composite Panels in the Post-Buckling Range," Firbrous Composites in Structural Design, Plenum Press, pp. 313~327.

Gibson, Ronald F., 1994, *Principles of Composite Material Mechanics*, Mcgraw-Hill, Inc., pp. 99~130.

Gurvich, M. R. and Pipes, R. B., 1995, "Probabilistic Analysis of Multi-Step Failure Process of a Laminated Composite in Bending," *Composite Science and Technology*, Vol. 55, No. 4, pp. 413~421.

Koiter, W. T., Elishakoff, I., Li, Y. W. and Starnes, J. H., 1994, "Buckling of an Axially Compressed Cylindrical Shell of Variablethickness," *International Journal of Solids and Structures*, Vol. 31, No. 6, pp. 797~805.

Lee, I. C. and Hong, C. S., 1996, "Buckling and Postbucking Behavior of Stiffened Laminated Composite Panels," *Trans. KSME* (in Korean), Vol. 20, No. 10, pp. 3199~3210.

Lin, S. C., T. Y. and Chu, K. H., 1998, "Evaluation of Buckling and First-Ply Failure Probabilities of Composite Laminates," *International Journal of Solids Structures*, Vol. 35, No. 13, pp. 1395~1410.

Stevens, K. A., Specht, S. and Davies, G. A. O., 1997, "Post-Buckling Failure of Carbon-Epoxy Compression Panels," *Proceedings of ICCM-11*, pp. 127~134.

Stevens, K. A., Ricci, R. and Davies G. A. O., 1995, "Buckling and Post-Buckling of Composite Structure," *Composites*, Vol. 26, pp. 189~199.

Stevens, K. A., Davies, G. A. O. and Ricci R., 1994, "Post-Buckling Failure of Composite Compression Panels," *19th ICAS Conference*, pp. 2975~2981.